RESEARCH ARTICLE | MAY 15 2019

Terahertz quantum cascade laser with non-resonant extraction

A. N. Baranov ; H. Nguyen-Van; Z. Loghmari; M. Bahriz ; R. Teissier

AIP Advances 9, 055214 (2019)
https://doi.org/10.1063/1.5092855

Terahertz quantum cascade laser with non-resonant extraction

Cite as: AIP Advances 9, 055214 (2019); doi: 10.1063/1.5092855
Submitted: 15 February 2019 • Accepted: 6 May 2019 •
Published Online: 15 May 2019

A. N. Baranov,[a] H. Nguyen-Van, Z. Loghmari, M. Bahriz, and R. Teissier

AFFILIATIONS

IES, Univ. Montpellier, CNRS, Montpellier, France

[a]Corresponding author, baranov@univ-montp2.fr

ABSTRACT

In order to improve the maximum operating temperature of THz quantum cascade lasers (QCLs) we propose to modify the three well resonant phonon design by increasing the energy of the separation between the bottom transition levels and the ground states, which is usually adjusted to the LO-phonon energy in GaAs. The fabricated devices based on this design with non-resonant depopulation of the bottom transition level operated in pulsed mode up to 190K, which is the best-reported performance for THz QCLs with $Al_{0.15}Ga_{0.85}As$ barriers based on an Au-Au double-metal waveguide. The performed analysis showed that the achieved improvement could be explained by the proposed design modification.

Quantum cascade lasers (QCLs) are very attractive sources of coherent radiation for spectroscopy in the THz domain because high power single frequency operation can be readily achieved. The first demonstration of THz QCLs in 2002[1] and the main milestones in the development of this technology covering now the spectral range of 1.2-5.4 THz[2–4] were achieved using the GaAs/AlGaAs material system. The drawback of THz QCLs is their low operating temperature, which requires using cooling equipment thus eliminating the advantage of the small size of these devices, and much effort has been put into increasing their maximum operating temperature T_{max}. After the first THz QCLs based on the chirped superlattice design[1,5] different variants of the bound-to-continuum[6] and resonant-phonon[7] designs were successfully used to fabricate THz QCLs. The three-well diagonal scheme with resonant LO-phonon depopulation of the bottom transition level was demonstrated to be the best suited for high temperature operation with T_{max} = 168 K achieved in lasers employing an Au-Au double-metal waveguide.[8] A Cu-Cu waveguide was proposed in the same publication in order to decrease losses in THz QCLs, which allowed the authors to reach T_{max}=178 K.[8] Different variants of the three-well design were examined to further improve T_{max}. In particular, the design was modified to increase the upper-level lifetime in order to obtain a higher gain and reduced parasitic leakage current[9] or to maximize the population inversion at high temperatures.[10] In combination with the Cu-Cu double metal waveguide these improvements resulted in the increase of T_{max} up to 186 K[9] and later to almost 200 K.[10]

In the THz QCLs the distance between the transition levels is smaller than the LO-phonon energy, which is favorable for achieving population inversion, but, at elevated temperatures, the energy of electrons in the upper level can be increased enough to make the emission of an LO-phonon possible.[2] This thermally activated LO-phonon scattering is the main reason of the low operating temperature of the existing THz QCLs. The efficiency of this mechanism is defined exclusively by the properties of the used materials and can be reduced in semiconductors with higher LO-phonon energies.[11] Another undesirable effect enhancing at elevated temperatures is the electron leakage into continuum states owing to the insufficient height of the AlGaAs barriers.[12] The influence of the AlGaAs barrier height on the QCL properties was studied in Ref. 13. An optimized structure employing AlGaAs barriers with 21% of Al exhibited a T_{max} = 191 and 196 K for the devices with the Au-Au and Cu-Cu waveguides, respectively.[13] Operation of a QCL at elevated temperatures is also affected by thermal population of the bottom transition level. The specific feature of the THz QCLs with resonant phonon depopulation consists in a fixed gap for this excitation, equal to the LO-phonon energy in GaAs (E_{LO} = 36 meV), which is necessary for fast electron extraction since any deviation from this value increases the bottom level lifetime. On the other hand, if this extraction gap is

larger the thermal backfilling can be reduced. This effect was noticed in Ref. 13 when considering the QCLs with different barrier heights. The Boltzmann factor BF = exp ($(e_{low}$-e0)/kT) describing the thermal backfilling varied between 0.158 and 0.097 at 200K in the structures with Al composition in barriers increasing from 12 to 24% but in the optimized design the energy separation in the phonon well was adjusted to match the LO-phonon energy for better depopulation of the bottom transition level.[13] In this work we present a study of a THz QCL based on the three-well design with the extraction energy gap exceeding the LO-phonon energy.

We modified the three-well resonant phonon design from[9] by increasing the extraction gap by 5 meV, up to 41 meV, while keeping the same shape of electron wavefunctions. Figure 1 presents the conduction band diagram and squared moduli of the wavefunctions computed using the in-house QCL simulation tool based on a one-band Shrödinger-Poisson solver that we successfully employed earlier for modelling of InAs/AlSb QCLs. The band diagram in Fig. 1 is calculated assuming a thermal equilibrium of the carriers within one period, without transport from one period to the adjacent ones. The band bending due to the charge of ionized donors and free electrons was taken into account in these calculations. The lasing transitions are e_4-e_2 and e_3-e_2. The operating electric field is higher than in the reference structure[9] because of the larger potential drop per period. The last well in the diagram is isolated from the next period of the structure for better visibility of the extraction gap. In the original design[9] the distance e_1-e_0 corresponds to the GaAs LO-phonon energy of 36 meV. The ground level e_0 is in fact splitted corresponding to a combination of the levels e_3 and e_4 of the previous wide well in the considered portion of the structure. Positions of the principal electron levels are shown in Fig. 2 as a function of applied electric field both for the original design and for the modified one where the distance e_1-e_0 was increased by 5 meV. We expect that this increase in the width of the extraction gap in our structure should result in reduction of the thermal backfilling. It can therefore be helpful for

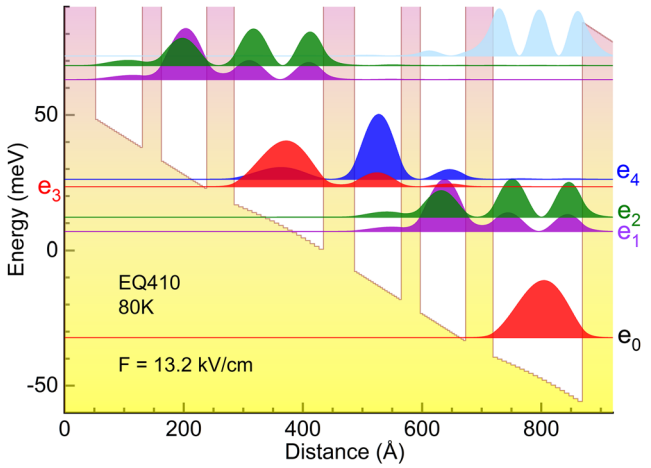

FIG. 1. Conduction band diagram and square moduli of electron wavefunction of the QCL design. The last quantum well is isolated from the next period of the structure for better visibility of the extraction gap e_1-e_0. The level e_0 is essentially the same as the level e_3 in the previous wide well.

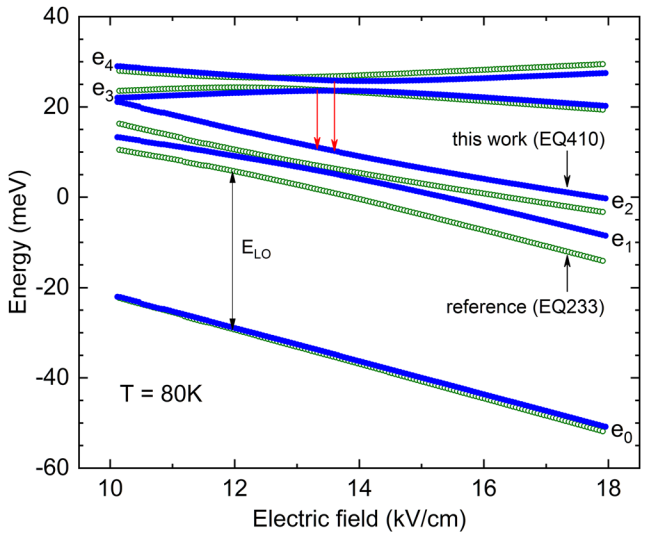

FIG. 2. Relative position of the energy levels in the QCL structure as a function of applied electric field. Red arrows show lasing transitions.

increasing the QCL operation temperature, provided the efficiency of the carrier extraction from the bottom transition level does not degrade much because of the deviation of the distance to the ground transition state from the LO-phonon energy. The goal of this work was to verify this assumption.

The GaAs/AlGaAs active zone of the QCL labeled EQ410 consisted of 300 repetitions of the following layer sequence **52**/78.5/**32**/76/**46**/150, in Å starting from injection barrier, $Al_{0.15}Ga_{0.85}As$ barriers in bold. A 12- Å -thick layer in the middle of the underlined barrier was doped with Si to 2.6 x $10^{17}cm^{-3}$ resulting in a sheet carrier density Ns = 3 x $10^{10}cm^{-2}$ per period. The structure was grown by molecular beam epitaxy in a RIBER 412 solid source machine on an undoped (100) GaAs substrate. The growth was started with a 300-nm-thick $Al_{0.55}Ga_{0.45}As$ stop etch layer. A 100-nm-thick GaAs bottom contact layer doped to n = 5 x $10^{18}cm^{-3}$ was grown before the laser active zone, and a 50-nm-thick GaAs top contact layer with the same doping level terminated the structure. The grown wafer was processed into (1-3)-mm-long and (120-150)-μm-wide ridge lasers with a double metal Au-Au waveguide. The devices were soldered with indium onto copper holders and mounted in a flow cryostat for measurements. The lasers were tested in pulsed mode using 333-ns-long current pulses at a repetition rate of 12 kHz. Light-current curves were measured using a slow pyroelectric detector and additional 20 Hz current modulation was applied in this case. Voltage-current and light-current characteristics of the best device are shown in Fig. 3. The laser threshold is clearly visible in the light-current curves presented in a linear scale up to a temperature of 185 K. Lasing was still observed up to T_{max} = 190 K but near this temperature the low output power and the vicinity of the NDR region did not allow clean recording of these pulsed characteristics. The threshold current density of the laser was 0.8 kA/cm^2 at 80K and increased up to 1.6 kA/cm^2 at the maximum operating temperature. T_{max} of several other devices fabricated from the same wafer was in the range 185-188 K.

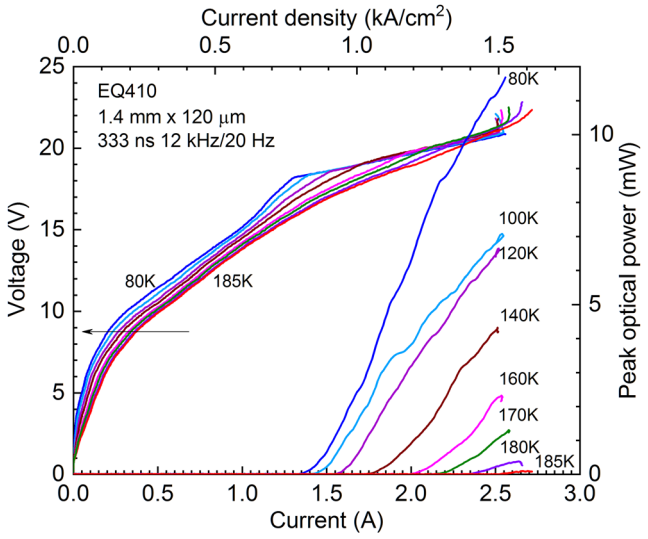

FIG. 3. Voltage-current and light-current characteristics of a QCL measured at different temperatures in pulsed mode (333 ns, 12 kHz/20 Hz). Optical power was measured at the exit of the cryostat without any correction for the collection efficiency.

Spectral measurements were performed using a Bruker Vertex 70 Fourier transform infrared spectrometer (FTIR) equipped with the pyroelectric photodetector. The FTIR was purged with dry nitrogen to eliminate strong absorption by water vapors in ambient air in the spectral region of interest. Emission spectra of the laser at 80K are presented in Fig. 4. for different currents. The emission frequency shifted from about 2.9 THz to 3.8 THz with increasing current (Fig. 4). It is worth pointing out a gap around 3.5 THz between the two observed group of longitudinal modes. The behavior of the emission spectra can be explained by analysis of the shift of electron level positions with applied electric field (Fig. 2). These results show that the low frequency emission at 2.9-3.3 THz is due to the e_3-e_2 transition (see also Fig. 1). At higher electric fields, the population of the e_4 level and the oscillator strength of the e_4-e_2 transition increase and this process becomes competitive or even dominating at high currents. The gap around 3.5 THz is due to the anticrossing of the levels e_4 and e_3. As it can be seen from Fig. 2, the e_3-e_2 separation increases faster with electric field than the e_4-e_2 energy, which explains the larger shift of the low frequency modes with current. The threshold current density of the laser increases with temperature faster than exponentially (Fig. 5). The straight dotted line in Fig. 5 shows a slope corresponding to characteristic temperature of 160 K for an exponential dependence. The laser emitted at 3.9 THz at 190K, which is shown in the inset in Fig. 5.

We compared the temperature behavior of the threshold current density of this laser and a reference QCL EQ233 based on the original design fabricated earlier. The active zone of this laser consisted of 300 periods of the same layer sequence **48**/85/**28**/85/**42**/164 (in Å) as it was employed in Ref. 9. This was the only difference of the devices fabricated from this wafer compared with the described above EQ410 lasers. Devices fabricated from both wafers exhibited similar performance at low temperature except the voltage that was about 2V lower at threshold in the lasers with the original design due to the smaller extraction gap. Above 140K the threshold current density of the reference laser grows faster and the operation temperature of the best devices is limited at 181 K (175-178 K, typically). This T_{max} is lower than it was achieved in Refs. 9 and 10 for lasers with a Cu-Cu waveguide but better than T_{max} = 168 and 180K demonstrated in Refs. 8 and 10, respectively, for QCLs of a similar three-well resonant phonon design with an Au-Au double-metal waveguide. Our QCLs with the large extraction gap and T_{max} = 190K

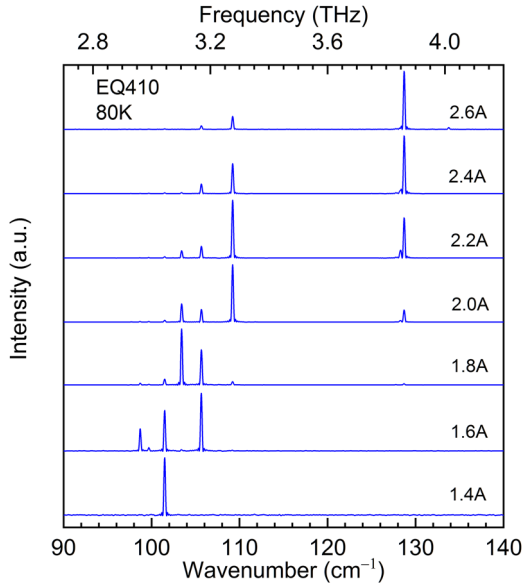

FIG. 4. Emission spectra of the QCL measured at 80 K at different currents.

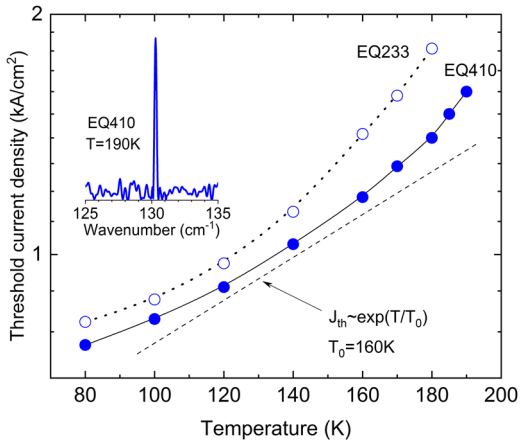

FIG. 5. Threshold current density of the EQ410 QCL as a function of temperature. Emission spectra of the laser at its T_{max} is presented in the inset. Dotted line shows data for a QCL EQ233 with the original design.[9] Laser dimensions: EQ410 – 1.4 mm x 120 μm, EQ233 – 1.2 mm x 140 μm. The straight dotted line showing a slope of an exponential dependence with T_0=160 K is given as a guide for the eye.

outperform all the devices based on the conventional three-well resonant phonon design with $Al_{0.15}Ga_{0.85}As$ barriers. The only better result of T_{max} = 191K, for THz QCLs with the Au-Au waveguide has been obtained in the lasers employing higher $Al_{0.21}Ga_{0.79}As$ barriers, which allowed reducing electron leakage into the continuum at elevated temperatures.[13] It should be noted that the QCLs with $Al_{0.15}Ga_{0.85}As$ barriers from the same work demonstrated T_{max} of only 163 K.

To estimate the effect of the design modification on T_{max} we should analyze the change in the carrier density in the bottom transition level e_2 due to the increase in the width of the extraction gap. The bottom transition level e_2 is populated by scattering of different origins from the upper e_3 and e_4 states characterized by the lifetime τ_2 and thermal excitation from underlying levels described by the Boltzmann factor. For simplicity we can consider that e_0 (Fig. 1) is the ground state that accumulate electrons with the density N_s and the thermal backfilling is governed by the distance e_1-e_0 that is equal to E_{LO} in the original resonant phonon design EQ233.[9] In the modified structure EQ410, the electron concentration n2 in the bottom transition level decreases because of the 5 meV increase in the energy of thermal activation and, in turn, increases due to a longer lifetime resulted from the deviation of the extraction energy from the resonance with E_{LO}. Using the Boltzmann factor the thermal population of e_2 can be estimated as $n2_{th}$ = 3.5 x 10^9 and 2.6 x 10^9 cm^{-2} at T = 200 K for the original design and the modified one, respectively, i.e., the change in $n2_{th}$ due to the larger extraction gap is $\Delta n2_{th}$ = -9 x 10^8 cm^{-2}. The electron concentration in e2 due to scattering from the upper levels e_3 and e_4 can be written as:

$$n2_{sc} = \frac{J}{q}\frac{\tau_{up}}{\tau_{up\to 2}}\tau_2$$

Where J is the current density, τ_{up} is the combined lifetime in the levels e_3 and e_4, $\tau_{up\to 2}$ is the lifetime of the transition between the combination e_3-e_4 and e_2, and q is the charge of electron. Considering that $\frac{\tau_{up}}{\tau_{up\to 2}} < 1$ one can conclude that

$$n2_{sc} < \frac{J}{q}\tau_2$$

The lifetime in level e_2 was calculated taking into account only the LO phonon scattering. Both emission and absorption processes were considered as presented in Ref. 14. The temperature dependence of the scattering rates comes from the equilibrium phonon occupation function 1/(exp(E_{LO}/kT)-1). We did not consider hot (non-equilibrium) phonons. The scattering to all other subbands was also taken into account, when allowed by energy conservation. Calculated values of τ_2 at 200 K are 0.30 and 0.33 ps for the structures EQ233 and EQ410, respectively. Finally, for the threshold current density of 1.8 kA/cm^2 at T = T_{max} we can deduce that the additional population of the level e_2 due to the increase of its lifetime in the modified design $\Delta n2_{up}$ is not greater than 3.4 x 10^8 cm^{-2}. Comparing $\Delta n2_{th}$ and $\Delta n2_{sc}$ and considering the assumptions made one can conclude that in the investigated structures the larger extraction gap can provide an improvement in the population inversion at elevated temperatures close to T_{max}. A more detailed analysis performed using our simulation tool and taking also into account the electron temperature that is typically 50-100 K above the lattice temperature qualitatively confirmed this conclusion.

The increase in τ_2 in the non-resonant design seems to be surprisingly weak, which makes interesting to explore this conclusion in more details. We estimated the effect of deviation of the extraction gap from the LO-phonon resonance on τ_2. The simulations included hot-LO-phonon scattering in emission and absorption processes. Instead of modifying design we varied the LO-phonon energy in simulations of both EQ233 and EQ410 structures in order to change the relative extraction energy. We believe that this much simpler approach gives a better visibility of the problem because it reflects only the effect of the extraction gap, which is not affected by the design features and operating conditions. Results of this simulation are presented in Fig. 6. The data at E_{ph} = 36 meV give the values corresponding to the conventional calculations. This analysis shows that the classical resonant phonon design is not so beneficial for depopulation of e_2 as it is usually expected. Faster electron extraction from the bottom lasing transition level can be achieved when the distance e_2-e_0 is equal to the LO phonon energy and not the distance e_1-e_0, as it is adjusted in the design. Another extremely important result consists in the weak dependence of τ_2 at high temperature on the deviation from the resonance, when the extraction gap is larger than E_{ph}. In such situation an additional increase in the extraction gap compared with the EQ410 structure seems to be helpful for further improvement of the population inversion at elevated temperatures and thus of T_{max}.

The data calculated for T = 80 K demonstrate a narrow LO-phonon resonance. Hence, in a design with a resonance at e_2-e_0 = 36 meV laser performances at low temperatures can be improved compared with the conventional approach,[9] since, in the absence of thermally activated mechanisms, the population inversion is inversely proportional to τ_2. A considerable increase in the gain can be expected at low temperatures for such design (Fig. 6) but at the expense of a lower T_{max}.

It is worth noting that the thermal backfilling in THz QCLs can be in principle suppressed by using a double-phonon resonant

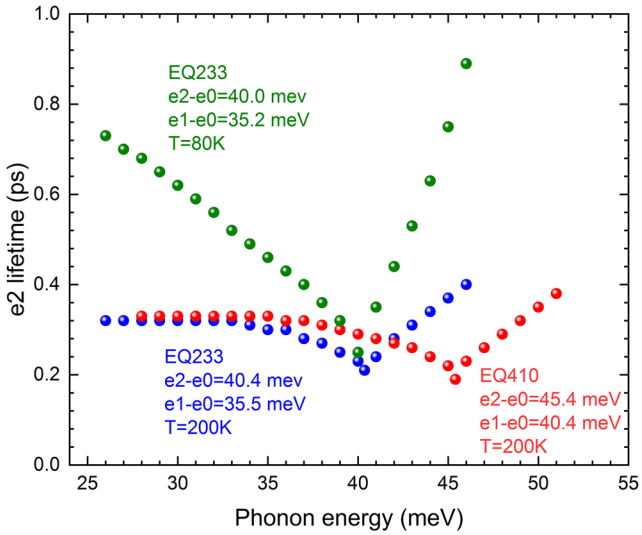

FIG. 6. Electron lifetime in the bottom level of the lasing transition e_2 as a function of the LO-phonon energy value used in calculations.

depopulation scheme where the energy separation between the bottom lasing level and the ground states is twice the LO phonon energy.[15] An improvement of T_{max} up to 172 K due to this approach was demonstrated in Ref. 16 but the current record performances were however achieved using the three-well design with a single-phonon depopulation.[9,10]

The problem of the optimal depopulation energy in the three-well design was considered in attempt to increase the depopulation rate of the bottom lasing transition level by activating different phonon modes in GaAs/AlGaAs heterostructures.[17] In a heterostructure, scattering takes place at energies close to LO-phonon resonances of both the well and barrier material. In THz QCLs, AlAs-like modes occurs around 47 meV in addition to GaAs-like phonons at 36 meV. Phonon scattering rates were calculated in Ref. 17 for three-well GaAs/$Al_{0.3}Ga_{0.7}As$ structures at T=10 K as a function of the depopulation energy varied between 30 and 60 meV considering both phonon modes or only the GaAs-like one. The performed analysis shows the goal cannot be achieved because the scattering rate practically does not change in the considered structures if the extraction gap is set to the energy of the AlAs-like phonons instead of usual 36 meV. Issues related to high temperature operation of such QCLs were not considered in this publication. These results demonstrate however, that the depopulation energy in the three-well design can be increased even more than we did in our work without a negative impact on the e_2 lifetime and thus the thermal backfilling can be further reduced.

In conclusion, we proposed to modify the three well resonant phonon design by increasing the energy of the separation between the bottom transition levels and the ground states above the energy of the GaAs LO-phonon in order to improve the population inversion at elevated temperatures and thus to increase the QCL operation temperature. This modification results in two competing processes: a decrease in the electron concentration at the bottom transition level because of the reduced thermal activation from the ground states and its increase due to a longer electron lifetime in the situation when the phonon resonance is broken. We demonstrated that the first mechanism can dominate. The fabricated devices based on such design with non-resonant depopulation of the bottom transition level operated in pulsed mode up to 190 K, which is the best-reported T_{max} for THz QCLs with $Al_{0.15}Ga_{0.85}As$ barriers based on an Au-Au double-metal waveguide. This value compares favorably with T_{max} = 181 K of the devices fabricated on the base of a conventional three-well design with resonant depopulation. The performed analysis showed that the achieved improvement could be explained by the proposed design modification. We believe that a combination of the proposed solution with the concept of high barriers,[13] and especially with a Cu-Cu waveguide will certainly helpful to further improve T_{max}.

Part of this work was supported by the French program "Investments for the Future" (EquipEx EXTRA (ANR-11-EQPX-0016) and IRN FIR-LAB.

REFERENCES

[1] R. Köhler, A. Tredicucci, F. Beltram, H. Beere, E. Linfield, A. Davies, D. Ritchie, R. Iotti, and F. Rossi, Nature **417**, 156 (2002).
[2] B. Williams, Nature Photonics **1**, 517 (2007).
[3] C. Walther, M. Fischer, G. Scalari, R. Terazzi, N. Hoyler, and J. Faist, Applied Physics Letters **91**, 131122 (2007).
[4] M. Wienold, B. Röben, X. Lü, G. Rozas, L. Schrottke, K. Biermann, and H. Grahn, Applied Physics Letters **107**, 202101 (2015).
[5] L. Ajili, G. Scalari, D. Hofstetter, M. Beck, J. Faist, H. Beere, G. Davies, E. Linfield, and D. Ritchie, Electronics Letters **38**, 1675 (2002).
[6] G. Scalari, L. Ajili, J. Faist, H. Beere, E. Linfield, D. Ritchie, and G. Davies, Applied Physics Letters **82**, 3165 (2003).
[7] B. Williams, H. Callebaut, S. Kumar, Q. Hu, and J. Reno, Applied Physics Letters **82**, 1015 (2003).
[8] M. Belkin, J. Fan, S. Hormoz, F. Capasso, S. Khanna, M. Lachab, A. Davies, and E. Linfield, Optics Express **16**, 3242 (2008).
[9] S. Kumar, Q. Hu, and J. Reno, Applied Physics Letters **94**, 131105 (2009).
[10] S. Fathololoumi, E. Dupont, C. Chan, Z. Wasilewski, S. Laframboise, D. Ban, A. Mátyás, C. Jirauschek, Q. Hu, and H. Liu, Optics Express **20**, 3866 (2012).
[11] G. Sun, R. Soref, and J. Khurgin, Superlattices And Microstructures **37**, 107 (2005).
[12] A. Albo, Y. Flores, Q. Hu, and J. Reno, Applied Physics Letters **111**, 111107 (2017).
[13] M. Kainz, S. Schönhuber, A. Andrews, H. Detz, B. Limbacher, G. Strasser, and K. Unterrainer, ACS Photonics **5**, 4687 (2018).
[14] T. Unuma and M. Yoshita, Journal of Applied Physics **93**, 1586 (2003).
[15] B. S. Williams, S. Kumar, Q. Qin, Q. Hu, and J. L. Reno, Applied Physics Letters **88**, 261101 (2006).
[16] R. W. Adams *et al.*, Applied. Physics Letters **93**, 131111 (2010).
[17] B. Williams and Q. Hu, Journal of Applied Physics **90**, 5504 (2001).